applied sciences

MDPI

Article

Geotechnical Evaluation of Diesel Contaminated Clayey Soil

Christian E. Hernández-Mendoza [1,*], Pamela García Ramírez [2] and Omar Chávez Alegría [2]

[1] CONACYT—Laboratory of Environmental Geotechnics, Facultad de Ingeniería, Universidad Autónoma de Querétaro, Circuito Universitario S/N, Querétaro 76010, Mexico
[2] Facultad de Ingeniería, Universidad Autónoma de Querétaro, Circuito Universitario S/N, Querétaro 76010, Mexico; carmenchis3@gmail.com (P.G.R.); omar.chavez@uaq.mx (O.C.A.)
* Correspondence: cehernandezme@conacyt.mx

Abstract: Soil contamination by different hydrocarbons has rapidly expanded worldwide, surpassing the self-purification capacity of soils and increasing the number of contaminated sites. Although much effort has been devoted to study the effects of diesel contamination on the geotechnical properties of soil, there is still limited available information about it. Moreover, there is no available information about the maximum diesel retention that soil can have and its effect on the geotechnical behavior of the soil. Thus, in this paper, we determined the maximum diesel retention by an unsaturated clayey soil and evaluated the impact of diesel contamination on its geotechnical properties. The results showed that the soil could only retain 12.6% of the added diesel and the excess was expulsed. At such a diesel concentration, the saturation rate of the soil was lower than 80%. Diesel contamination increased the plasticity and the internal friction angle of the soil, while its cohesion was considerably decreased. It should be noted that the matric suction of contaminated soil was lower than the one obtained for natural soil. However, its osmotic suction was considerably higher. This indicates that osmotic suction must be considered to evaluate the shear strength of contaminated soils.

Keywords: geotechnical properties; diesel; contaminated soil; clay; environmental geotechnics

Citation: Hernández-Mendoza, C.E.; García Ramírez, P.; Chávez Alegría, O. Geotechnical Evaluation of Diesel Contaminated Clayey Soil. *Appl. Sci.* **2021**, *11*, 6451. https://doi.org/10.3390/app11146451

Academic Editor: Daniel Dias

Received: 10 June 2021
Accepted: 9 July 2021
Published: 13 July 2021

1. Introduction

Hydrocarbons are the main energy source used to satisfy our energy needs, but during their life cycle, they can produce many environmental impacts. Hydrocarbon leaks/spills, which can occur from its exploitation to use, cause environmental pollution, where, commonly, the first receptor is the soil.

Soil contamination by hydrocarbons can be originated by accidental spills during its transportation and disposal, leakage of storage tanks and pipes, and/or by clandestine fuel intakes. The unsaturated (aerated) zone of the soil, that is, the area in which the infrastructure's foundations are frequently laid, is the first one to be contaminated by hydrocarbon leaks and/or spills.

It is also possible that hydrocarbons permeate through the soil up to the groundwater level zone, contaminating the saturated zone of soil. Therefore, hydrocarbon leaks and spills can affect the deep foundations located on it as well as it can contaminate groundwater. In this case, the hydrocarbons can be transported by the groundwater to the surrounding areas contaminating the soil and may affect the foundations located in such areas.

The permanence of hydrocarbons in the unsaturated zone depends on different factors, such as the solubility, volatility, toxicity, biodegradation rate, and sorption of the hydrocarbons; the nature and permeability of the soil or soils forming the unsaturated zone; and the natural or man-made liquid flow (water and/or contaminants).

Unfortunately, soil contamination by different hydrocarbons has rapidly expanded worldwide, surpassing, in many cases, the self-purification capacity of soils. As a result, the number of hydrocarbon-contaminated sites has increased in both developed and developing countries, latter being the more affected ones.

Soil is the most frequent source of risk to construction projects [1] due to not only the geotechnical or geological aspects but also the contaminants present in it. Nevertheless, there is still limited available information about the impact of hydrocarbons contamination on the geotechnical properties of the soils. Some of the risks associated with soil contamination are loss of foundation and structural integrity, damage to construction materials, and loss of facility [1]. Independent from the time the soil gets polluted—before or after the infrastructure construction—the changes caused in its engineering properties can place both the integrity of the structures and its users at risk.

It is known that soil contamination by hydrocarbons affects its engineering properties. However, such an effect depends on many variables, such as the type of soil and the physical and chemical properties of the spilled/leaked hydrocarbon [2–4].

Published papers have been focused on the effect of diesel contamination on the geotechnical properties of soil by varying the contaminant concentration from 0% to 20% (weight basis) [5–9]. However, none of them has been focused on the quantity of diesel that soil is capable to retain. This can have important repercussions since the exceeding hydrocarbons can be subjected to evaporation or transportation depending on the type of hydrocarbon and the local environmental conditions. Nevertheless, the retained hydrocarbons can have a major influence on the geotechnical behavior of the contaminated soil.

Izdebska-Mucha and Trzcinski [10] reported that after contaminating a clay sample with diesel, clay particles showed a change in their microstructure, resulting in a denser structure due to change in the pore size distribution. Ijimdiya [4] studied the effects of used motor oil on the properties of lateritic soil and found a reduction in the amount of fine-grained size particles of the soil as the concentration of the contaminant was increased from 0% to 8%.

Son et al. [11] estimated the effect of diesel contamination on the electrical properties of unsaturated soils. These authors reported that contaminated soils with a water content of 5% had higher electrical resistivities and decreased permittivity compared to uncontaminated soils. In contrast, contaminated soils having a water content of 15% showed smaller resistivities and higher permittivity compared to non-contaminated soils.

It has been reported that soil contamination affects its consistency limits. Salimnezhad et al. [12] reported that the plastic limit of a crude-oil-contaminated soil increased as the contaminant concentration increased, but the plastic index decreased as the contaminant concentration increased. Yazdi and Teshnizi [7] found that the liquid limit of a gasoline-contaminated soil increased, reaching maximum value at a contaminant concentration of 6%. Although a further increase of gasoline concentration reduced the liquid limit of the soil, it was higher than the one obtained for the natural soil.

Salimnezhad et al. [12] reported that swelling pressure of natural soil was higher than that of contaminated soil. However, for 12% oil content, the contaminated soil had a higher free swell percentage than the natural soil.

Other researchers have studied the effects of diesel [5], oil [13], gasoline [6], and crude oil [12] on the shear resistance of different clay soils, finding that soils' cohesions tended to decrease as the contaminant concentration increased. However, while in some cases, the internal friction angle was reported to increase as the contaminant concentration increased [5,6], in other cases, a reduction of its value was reported as the contaminant concentration increased [7,12,13]. These results may mean that clay minerals exhibit different behaviors according to the hydrocarbon used to contaminate the soil.

Yazdi and Teshnizi [7] showed that the settlement and ductility of a gasoline-contaminated soil increased as the contaminant concentration increased. They also found that the soil failure mechanisms changed depending on the contaminant concentration in the soil.

Taheri et al. [9] studied the effects of soil contamination in a soil that was simultaneously contaminated with lead and diesel. These authors found that the increase in diesel concentration reduced the hydraulic conductivity of the contaminated soil. Such

decrease was because diesel occupied the pore spaces and limited the water flow through the soil samples.

Salimnezhad et al. [12] found that the settlement of the contaminated soil increased as the crude oil concentration increased because the contaminant reduced the specific surface area of the soil, decreasing the water absorption of the particles of the soil facilitating the water drainage.

Although many efforts had been carried out to study the effects of diesel contamination on the geotechnical properties of soils, most of the studies had focused on saturated soil conditions. As a result, the available information about the effect of diesel contamination on unsaturated soils is scarce. Moreover, to the widest knowledge of the authors, there is no available information about the maximum diesel retention that natural soil can have and its effect on the geotechnical behavior of the soil.

Thus, the objective of this study was to determine the maximum diesel retention by an unsaturated clayey soil, and to evaluate the impact of diesel contamination on its geotechnical properties. The test performed in both natural and contaminated soil conditions showed that although the soil could not retain more diesel, its saturation rate did not exceed 80%. Furthermore, the changes in the geotechnical properties of the contaminated soil promoted an increase in its shear strength resistance. Such difference was due to an increase in the osmotic suction in the contaminated soil.

2. Materials and Methods

2.1. Experimental Procedure

The experiment was performed in two phases: natural soil characterization and soil contamination and characterization. In the first phase, the extraction of disturbed natural (uncontaminated) soil samples from a place in the north of Querétaro City, Mexico, was done. An undisturbed cubic soil sample was extracted to evaluate the natural soil's water content and volumetric unit weight. All soil samples were stored in a controlled temperature chamber (20 ± 1 °C) until its use for geotechnical characterization.

All the disturbed soil samples were mixed into the controlled temperature chamber to obtain a uniform mass of soil to perform the remaining geotechnical tests. This soil mass was divided into subsamples, poured into hermetically sealed containers, and stored in the same chamber. The soil sample quantity that is required for each test could now be taken with ease, avoiding opening and manipulating the whole soil sample every time a quantity of soil was needed for analysis.

The tests were performed according to the methods described in the Test Methods section. The unit weight of the natural soil was $\gamma_m = 15.10$ kN/m^3 $\pm$ 0.10 kN/m^3, and its water content was $w = 36.94\% \pm 0.19\%$; this corresponded to an average saturation rate of $s_r = 70.82\% \pm 0.18\%$. After finished the natural soil characterization, the soil contamination process was started.

In the second phase of this work, the remaining soil sample was contaminated with diesel for its geotechnical characterization. Table 1 shows the characteristics of the commercially available diesel used to contaminate the soil. To define the quantity of diesel needed for soil contamination, a 50-g natural soil sample was placed in a sealed glass container. Then, this soil subsample was contaminated with diesel, at an initial concentration of 4% by weight, and stored for seven days in the temperature-controlled room.

During this curing period, the contaminant could distribute throughout the soil and react with the pore fluid to achieve ionic stability [2]. After the curing period, the sample was visually inspected to verify if the soil could retain the added diesel. This process was repeated by increasing the diesel concentration (i.e., 4%, 8%, 12%, and 14%) until the soil could not retain more diesel.

Table 1. Applied diesel fuel specifications [14].

Parameter	Value
Flash point (°C)	≥45
Density (kN/m^3)	8.16
Specific gravity	0.832
Kinematic viscosity at 40 °C (mm^2/s)	1.9–4.1
Cetane index	≥48
Sulfur content (ppm)	<500
Aromatics content (%, in volume)	≤30
Water and sediments (%, in volume)	≤0.05

When the soil could not retain more diesel, it was transferred to a smaller glass container to allow the soil to drain the exceeding contaminant. Then, a contaminated soil subsample was taken from the top of the container to determine the retained diesel concentration by a gravimetric method [15]. The retained diesel concentration was 12.62% ± 0.27%. Therefore, such a concentration of diesel was used to contaminate the natural soil to be used during this second phase.

Once the diesel concentration to contaminate the soil was defined, the following procedure was applied. First, the remaining natural soil was air-dried to reduce its water content. This was done because in the previous experiment, a considerable increase in the liquids content of the contaminated soil was noticed (see Section 3.1). Then, the soil was placed in a container to mix it manually with diesel to simulate the long-term contamination effect [16].

Next, the contaminated soil was poured into hermetically sealed containers and stored in the temperature-controlled room for six weeks. After this curing period, the contaminated soil was tested as indicated in the Test Methods section.

The selected contamination procedure is an alternative way to reduce the sample preparation time [16]. It also allows the contaminant to bring about a long-term change in the initial soil structure [16]. Although a curing time of seven days is enough to allow the soil to react with the contaminant [2], the curing period was extended to six weeks to enhance the long-term contamination effect.

2.2. Test Methods

The evaluated properties of the soil are summarized in Table 2 and were executed as indicated in the corresponding standards. The "water content" of the contaminated soil was obtained by applying the same standard used for the natural soil. However, the term "water content" was transformed to "liquids content" to consider the difference in specific gravity between diesel and water [17].

To determine the modified free swell index (MFSI) for both soil conditions, 10 g of oven-dried (105 ± 1 °C) soil passing a No. 40 (425 µm) sieve were poured into a 100-mL graduated cylinder filled with distilled water. The soil was manually mixed with the distilled water and left undisturbed for the soil to swell/settle and achieve an equilibrium state of volume. The MFSI was calculated as the ratio of the equilibrium sediment volume to the dry weight of the oven-dried soil.

The liquid limit was evaluated by the fall cone method as indicated in the standard procedure adopted. Distilled water was gradually added to the soil—both natural and contaminated—to obtain a semiliquid consistency. The soil and the added water were thoroughly mixed until a homogeneous mass was obtained. This mass was poured into a sealed container. It was stored in the controlled-temperature chamber for 24 h to allow the added water to permeate through the soil before the cone penetrometer tested the sample. For both soil conditions, the liquid limit was evaluated by considering the equivalent water content of the samples.

The direct shear test was executed in a 100 mm × 100 mm shear box at a shear velocity of 1 mm/min. Normal stresses applied were 50, 100, and 200 kPa. Matric and total suction

of the soils were evaluated by the filter paper method, using the calibration curves for wetting the filter paper, Whatman No. 42.

Table 2. Evaluated properties of both natural and diesel contaminated soils.

Property	Method Applied
Water content [1]	ASTM D2216 [18]
Unit weight	ASTM D7263 [19]
Soil mineralogy	X-ray diffraction analysis
Chemical elements analysis	Total reflection X-ray fluorescence spectroscopy
Specific gravity of soil solids	ASTM D854 [20]
pH	NOM-021-RECNAT-2000 [21]
Particle-size distribution of soil	ASTM D6913 [22], ASTM D1140 [23]
Liquid limit and plastic limit	BS EN ISO 17892-12 [24]
Soil classification	ASTM D2487 [25]
Modified free swell index	Sridharan and Rao [26]
Direct shear	ASTM D3080 [27]
Soil suction	ASTM D5298 [28]
Soil texture	NOM-021-RECNAT-2000 [21]
Electrical conductivity	NOM-021-RECNAT-2000 [21] (by the saturated paste extract, soil to water ratio of 1:2.5)
Organic content	AASHTO T 267 (by loss-on-ignition) [29]
Cation exchange capacity	NOM-021-RECNAT-2000 (Kjendahl method) [21]

[1] As a technical precision, in the case of the contaminated soil, the term "water content" was replaced by the term "liquids content" [17].

The pH and the electrical conductivity (EC) of the soils were measured with a pH/EC/DO/ISE multiparameter (Orion Versa Star Pro, Thermo Scientific, Waltham, MA, USA) with automatic temperature compensator, equipped with a glass electrode for pH measurements and an EC sensor. Before each natural and contaminated soil sample set's pH measurement, the equipment was calibrated with the traceable to the National Institute for Standards and Technology (NIST) buffer solutions of pH 4, pH 7, and pH 10 obtained from Thermo Fisher. The equipment calibration was repeated until a correlation coefficient of the calibration curve of the multiparameter was at least of 0.98. For the EC measurements the equipment was calibrated with the traceable to NIST standard solutions of 100 µS/cm and 1413 µS/cm obtained from Thermo Fisher (Austin, TX, USA).

2.2.1. Chemical Elements Analysis of the Soil

The elemental chemical characterization of soils was performed with a total reflection X-ray fluorescence spectroscope (S2 PICOFOX TXRF, Bruker Nano), equipped with a molybdenum tube and silicon drift detector. The S2 PICOFOX is a portable benchtop spectrometer for multi-element analysis of liquids, suspensions, and solids.

Before analysis of the samples, a gain correction was performed with a mono-element standard sample (1 µg As). Further, the spectroscopic resolution (1 µg Mn) and sensibility analysis (1 ng Ni) of the spectroscope were performed according to the manufacturer instructions.

The standard solutions of H_3AsO_4 (1000 mg/L); SiO_2 (10,000 mg/L), $Ni(NO_3)_2$ (1000 mg/L); $Fe(NO_3)_3$ (1000 mg/L); $Al(NO_3)_3$ (10,000 mg/L); $Ca(NO_3)_2$ (10,000 mg/L), $NaNO_3$ (10,000 mg/L), KNO_3 (10,000 mg/L), $(NH_4)_2TiF_6$ (1000 mg/L), $Mg(NO_3)_2$ (10,000 mg/L), $Mn(NO_3)_2$ (10,000 mg/L), and $Zn(NO_3)_2$ (10,000 mg/L) were obtained from Merck, with a quality for Inductively Coupled Plasma (ICP) test, traceable to the Standard Reference Material (SRM) from NIST. The necessary dilutions have been made from the stock solutions in order to achieve the linearity of the standard curve.

The soil samples for elemental analysis were prepared as follows: 20 mg of soil was ground in an agate mortar and then passed through a No. 230 (63 µm) sieve. Then, the powder was suspended in 1 mL of dispersant solution (1% Triton X-100 in distilled water).

The soil suspension was spiked with 10 µL of gallium (1000 mg/L, ICP standard traceable to SRM from NIST, Sigma Aldrich, St. Louis, MO, USA) as internal standard.

The suspension was then sonicated for 15 min, after which it was homogenized in a vortex agitator. Then, 10 µL of a sample solution was transferred into a siliconized quartz glass sample carrier and dried at 50 °C on a hot plate. The prepared soil samples were analyzed with a live collection time of 1000 s. Spectra acquisition and data evaluation were done by using the software Spectra 7.8 (Bruker Nano GmbH, Berlin, Germany).

2.2.2. Cation Exchange Capacity of the Soil

The cation exchange capacity (CEC) of the soil was evaluated according to the Mexican standard NOM-021-RECNAT-2000 [21], using ammonium acetate (1N, pH 7, American Chemical Society grade, Meyer) as a saturating solution to replace the absorbed cations (Ca^{2+}, Mg^{2+}, Na^{+}, and K^{+}). Firstly, the soil was air-dried and sieved through the No. 10 (2 mm) sieve. Then, the exchange complex was saturated with the ammonium cation. After that, the ammonium cation was removed with a sodium chloride (NaCl, American Chemical Society grade, Merck) solution and the total capacity change was determined (Kjendahl method). The detection limit for the total CEC was 3.86 $cmol_{+}/kg$.

2.2.3. Soil Mineralogy

Soil samples were powdered in an agate mortar and sieved through a No. 200 sieve. The powders were characterized by X-ray diffraction (XRD Rigaku, MiniFlex) with Cu-Kα radiation (λ = 1.5406 Å). Diffraction intensity, in function of 2θ, was analyzed at the interval from 2° to 80°, with a 2θ step size of 0.02°, and a counting time of 0.06 s per point. Interplanar spaces (d) were evaluated by the Bragg's law equation:

$$n\lambda = 2d\ \sin(\theta) \quad (1)$$

where n is the class of diffraction peak ($n = 1$ for the first-order basal reflection), λ is the Cu-Kα wavelength of the incident X-ray wave, and θ is the diffraction angle.

3. Results and Discussion

3.1. Diesel Retention in the Contaminated Soil

At 4% diesel concentration, the natural soil readily absorbed the contaminant (Figure 1b). In contrast, at 14% diesel concentration, the soil could not retain the contaminant at all (Figure 1c). After analyzing the contaminated soil, it was found that the soil retained only 12.62% ± 0.27% of diesel.

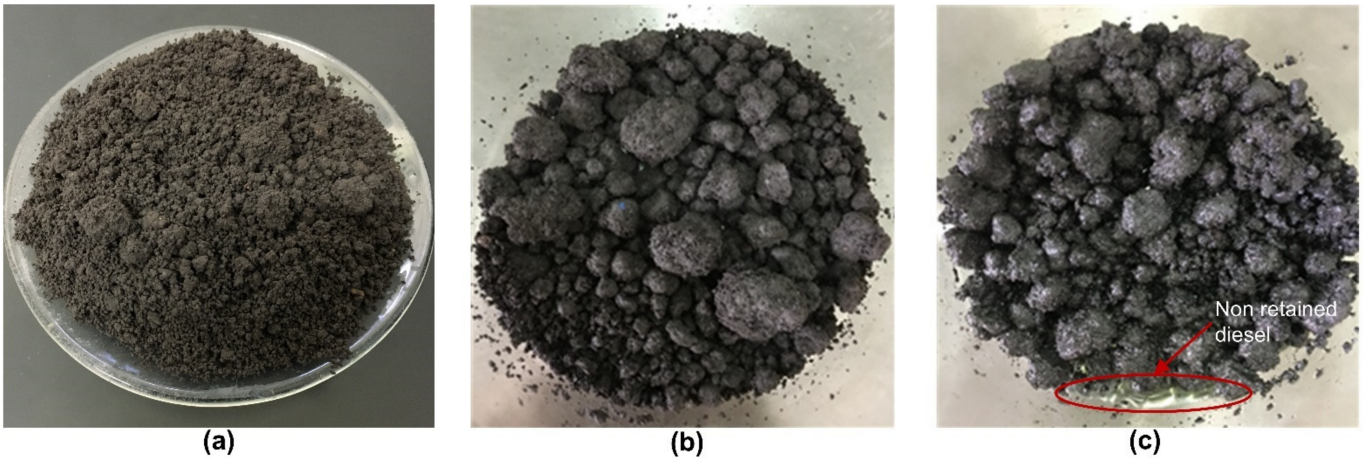

Figure 1. Evolution of soil aspects as diesel concentration increased from: (**a**) natural soil, (**b**) 4% added diesel, and (**c**) 14% added diesel.

Clay fractions of soil can adsorb non-polar molecules—such as diesel—due to the van der Waals attraction forces [30]. Such attraction forces between particles rapidly decay with the surface-to-surface distance (varying inversely as the seventh power of distance between the plates). However, attractive forces are additive. So, van der Waals attraction forces can be calculated by adding the attractions among all the particles. This may result in a higher total force and a lower decay (varying inversely as the third power of distance between the plates) with the surface-to-surface distance [30].

Nonetheless, Anandarajah and Chen [31] found that van der Waals attraction forces get reduced when fluid other than water fills the medium between the attracted particles. Further, Chiou and Shoup [32] showed that organic compounds that are not potent wetting agents have lower sorption capacity on polar mineral surfaces [32]. Hence, this makes water a stronger opponent to displace non-ionic organic solutes from minerals in aqueous systems.

In the absence of water, clay particles can behave as conventional organic compound absorbers, its large surface area being the main contributor to its high absorptive capacity [33]. However, in the presence of water, the absorption of non-polar hydrocarbons can be suppressed since non-polar organic molecules are not solid competitors for adsorption sites on the clay surface compared to highly polar water [30].

Thus, in the present study, since the soil was contaminated at its natural water content, diesel adsorption by the soil minerals was limited to those places where soil absorption sites were available. This means that soil could only retain the required diesel to satisfy its hydration needs.

Diesel is a non-polar mixture of aromatic (including naphthalenes) and saturated (including isoparaffins and cycloparaffins) hydrocarbons obtained from petroleum. Diesel hydrocarbons have carbon numbers in the range of C9–C28 with high boiling points between 170 and 430 °C. As previously stated, the term "water content" was transformed to "liquids content" to consider the difference in specific gravity between diesel and water [17]. Thus, Equation (2) was used to consider the contribution of the liquid's specific gravity on the liquids content of the soil [17].

$$E_{wc} = l_c \left(\frac{c+1}{c+G_f} \right), \tag{2}$$

where E_{wc} is the equivalent water content, l_c corresponds to the liquid content, c is the water to diesel volume ratio in the pore's liquid, and G_f is the specific gravity of diesel. It must be mentioned that in Equation (2), for water that has not been mixed with any contaminant, $c = 0$.

Table 3 presents the impact on the E_{wc} and the saturation rate (s_r) of the soil due to its contamination. Diesel contamination increased the E_{wc} and the s_r of the contaminated soil by 18% and 12%, respectively, compared to the natural soil. Such an increase in both parameters influences the engineering behavior of the contaminated soil. It can even make it complicated to directly compare the results obtained by both soil conditions.

Table 3. Change in soil's saturation rate due to diesel contamination.

Parameter	Natural Soil	Contaminated Soil
Water content, w (%)	36.94 ± 0.19	- - - -
Liquids content, l_c (%)	- - - -	42.54 ± 1.21
Water to diesel volume ratio, c	0	6.94
Equivalent water content, E_{wc} (%)	36.94 ± 0.19	43.46 ± 1.21
Saturation rate, s_r (%)	70.82 ± 0.18	79.46 ± 1.03 [1]

Values in the table: mean value ± standard deviation (n = 3). [1] The s_r of the contaminated soil was calculated using E_{wc} instead of w.

Hence, we decided to air-dry the natural soil before its contamination and then add the diesel to achieve a concentration of 12.62%. Hence, the contaminated soil used for its characterization had a liquids content ($l_c = 34.39 \pm 0.22\%$), equivalent water content ($E_{wc} = 35.13 \pm 0.22\%$), and saturation rate ($s_r = 71.28 \pm 0.21\%$) closer to the same factors observed in the natural soil.

3.2. Influence of Diesel Contamination on the Soil's pH

Soil contamination with diesel had a significant impact on its pH. After soil contamination, the pH of the soil changed from moderately alkaline ($pH_{natural} = 7.95 \pm 0.14$) to neutral ($pH_{contaminated} = 6.98 \pm 0.03$). Nevertheless, this pH drop does not represent a limitation for biodegradation processes, since the pH for the biotransformation of the contaminant has been found to be in the range of 6 to 8 [34]. This tendency to decrease the pH as the soil gets contaminated agrees with the results obtained by Taheri et al. [9].

The pH reduction of soil after its contamination was due to the acidifying effect of the sulfur contained in diesel. It is known that the addition of elemental sulfur (S) to soil affects the oxidation rate and produces two hydrogen ions due to the microbial activity of soil (Equation (3)). Since pH is a measure of the hydrogen ion concentration ($pH = -\log_{10}[H^+]$) in soil solution, the increase in concentration resulted in a lower pH.

$$S + CO_2 + \frac{1}{2}O_2 + 2H_2O \rightarrow CH_2O + SO_4^{2-} + 2H^+ \quad (3)$$

Momeni et al. [35] studied the effect of acid and alkaline waters on the geotechnical properties of clay soil and found that the decrease of the pH value of the soil increased the liquid limit and the plastic index of the soil. Moreover, they indicated that the coefficient of permeability of the soil increased as the pH values of the soil shifted from the neutral condition to the acidic or alkaline conditions [35].

3.3. Influence of Diesel Contamination on the Soil's Texture

Diesel contamination of natural soil caused a change in its texture classification from silty clay to silty loam. This change, from a fine texture to a ridged one after soil contamination, was due to the agglomeration of soil particles as a response to soil acidification and the reduction of the dielectric constant of the pore fluid.

A decrease in pH promoted the exchange of calcium ions by hydrogen ions, which resulted in clay particle agglomeration/flocculation due to its surface charge alteration [36]. Furthermore, partial replacement of water contained in the pores of soil by the contaminant changed the dielectric constant value of the pore fluid. Hence, the attractive forces prevailed over repulsive ones, resulting in soil agglomeration/flocculation [37].

The van der Waals attraction force developed between two parallel plates can be calculated as shown in Equations (4) and (5), while the repulsion force can be obtained as indicated in Equations (6) and (7) [37].

$$Att = \frac{H}{6\pi d^3}, \quad (4)$$

where d is the distance between plates and H is the Hamaker constant obtained as follows [37]:

$$H = \frac{3}{4}kT\left(\frac{\varepsilon_1 - \varepsilon_2}{\varepsilon_1 + \varepsilon_2}\right)^2 + \frac{3h\nu_e}{16\sqrt{2}}\frac{\left(m_1^2 - m_2^2\right)^{3/2}}{\left(m_1^2 + m_2^2\right)^{3/2}}, \quad (5)$$

where k is the Boltzmann constant, T is the absolute temperature, ε_i denotes the dielectric constant of the medium, h is the constant of Planck, ν_e corresponds to the main electronic adsorption frequency in ultraviolet light, and m_i is the reflective index of the medium in visible light.

$$Rep \propto \frac{1}{K_1\beta}, \quad (6)$$

where K_1 is a constant that depends on the valence of the ions and the ionic concentration and β can be obtained as follows [37]:

$$\beta = \frac{K_1}{\varepsilon k T K_3}, \quad (7)$$

with K_1 and K_3 being constants that depend on the ionic concentration.

It can be appreciated from Equations (4) and (6) that both attractive and repulsive forces depend on the dielectric constant value of the pore fluid. However, the variation of the dielectric constant value of the pore fluid has a higher effect over the repulsive forces [37]. Thus, a decrease on the value of the dielectric constant of the pore fluid reduced both attractive and repulsive forces, but the decrease in repulsive forces was bigger than the decrease in the attractive forces. Hence, attractive forces prevail over repulsive ones (the net effect was attractive) and gave as result the agglomeration of the soil particles.

3.4. Effect of Diesel Contamination on the Specific Gravity of Soil

The specific gravity of natural soil was reduced from 2.72 ± 0.02 to 2.60 ± 0.02 after soil contamination with diesel. The partial substitution of water (in the contaminated soil) explains this significant change ($p < 0.01$) since diesel has a density and specific gravity lower than water.

3.5. Impact of Diesel Contamination on the Soil's Particle Size Distribution

Grains' size content of both soils is presented in Table 4, and their granulometric curves are shown in Figure 2. Both natural and diesel contaminated soils corresponded to a fine-grained soil. After diesel soil contamination, a significative ($p < 0.01$) change in fine-grained particles sizes' content was observed. The silt-like sized granules increased by 37% while the clay-like sized granules decreased by 46%. This change was due to both the reduction of the dielectric constant and the acidification of the pore fluid of the soil, which caused that the clay-like sized particles agglomerated and increased their size reaching a silt-like size.

Table 4. Impact of diesel contamination in grain-like size distribution of soil.

Grain Size	Natural Soil	Contaminated Soil
Gravel (%)	0.25 ± 0.06	0.22 ± 0.03
Sand (%)	7.34 ± 0.49	6.43 ± 0.21
Silt (%)	52.03 ± 1.21	71.72 ± 1.44
Clay (%)	40.38 ± 2.30	21.63 ± 0.70

Values in the table: mean value ± standard deviation ($n = 5$).

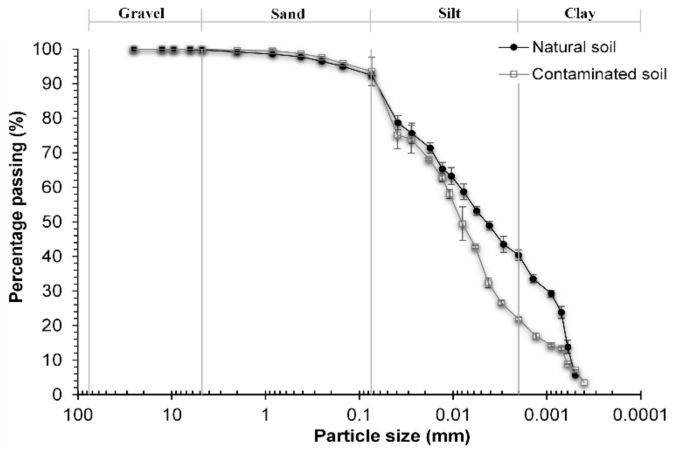

Figure 2. Impact of diesel contamination on particle size distribution of soil. Error bars denote standard deviations.

Lambe and Withman [38] indicated that the reduction of the dielectric constant and/or pH drop, as well as ion valence reduction and/or electrolyte concentration decrease, promotes soil flocculation. In low pH environments, the thickness of the double layer around clay particles can decrease [39]. The diffuse double layer theory indicates that the thickness of the double layer ($1/\chi$) can be calculated as indicated in Equation (8):

$$\frac{1}{\chi} = \sqrt{\frac{\varepsilon kT}{8\pi z^2 e^2 \eta}} \quad (8)$$

where ε corresponds to the dielectric constant of the pore fluid, k is the Boltzman constant, T is the absolute temperature, z is the valence of the cations, e is the electric charge, and η is the concentration in number of ions per milliliter.

When the soil was contaminated with diesel ($\varepsilon_{diesel} = 2.3$), it interacted with the water ($\varepsilon_{water} = 80.3$) contained in the pores of the soil and reduced the dielectric constant of the pore fluid. As a result, the thickness of the double layer was reduced and the soil particles began to join together due to the influence of the van der Waals forces. As the soil particles got closer to each other, the effect of the van der Waals attractive forces increased. This promoted the agglomeration of clay particles by forming flocs, which was appreciated as an increment in the silt-like size fraction content, with a correspondent decrement in the clay-like size fraction.

3.6. Influence of Diesel Contamination on the Consistency Limits

Table 5 provides the plastic characteristics of the soils. According to their Atterberg limits, both the natural and the contaminated soils are considered as very high and expansive ones. Despite the variations of the values of the Atterberg limits, both the natural and the contaminated soils were classified as silts of high compressibility. The natural soil was considered as a normal active clay, while contaminated soil was considered as a very active one. This increase in the activity of contaminated soil, in comparison with its activity at uncontaminated condition, was attributed to the physical and chemical effect of diesel on clay particles.

Table 5. Influence of diesel contamination in the consistency limits of soil.

Parameter	Natural Soil	Contaminated Soil
Liquid limit (%)	77.3 ± 0.4	83.9 ± 1.9
Plastic limit (%)	35.8 ± 2.2	37.3 ± 1.0
Plasticity index (%)	41.5 ± 2.5	46.7 ± 1.5
USCS classification	MH	MH
Average clay activity (%) *	1.03	2.14

Values in the table: mean value ± standard deviation (n = 5). * Calculated as: average plasticity index/average clay fraction.

After soil contamination, its liquid and plastic limits increased by 9% and 4%, respectively. It is known that the liquid behavior of soils is influenced by free water, which is not absorbed by the particles of soil and can freely move through soil pores. When diesel was added to the natural soil, it covered the surfaces of the clay particles, making the contact between the free water and the clay particles more difficult.

Since diesel is a non-polar liquid, it could not allow that the water added during the test, which created a link with clay surface, to provide the required condition for clay to flow. When water was added to the contaminated soil to evaluate its Atterberg limits, it gradually displaced the diesel adhered to clay surface, allowing the interaction between clay and water. Thus, more water was needed in the contaminated soil to achieve its plastic state and, thus, higher plasticity was obtained.

3.7. Effect of Diesel Contamination on the Modified Free Swell Index of the Soil

The MFSI test classified the natural soil as a high-swelling potential clay (2.33 ± 0.47 cm^3/g). However, this index classified contaminated soil as a very high-swelling potential soil (3.79 ± 0.77 cm^3/g). This finding agrees with those reported by Salimnezhad et al. [12], who observed an increase in the free swelling of oil-contaminated clayey soil as the contaminant concentration increased from 4% to 12%.

At low pH levels, acids attack the original minerals contained in soil and produce a modification in both the silica and alumina content, reducing the Si/Al ratio as well as the calcium content (see Table 6). Hence, the chemical composition of the soil changed when the pH of the pore fluid diminished, and due to the reduction of the calcium content there was an increase in its swell capacity.

Table 6. Impact of diesel contamination on the concentration of the chemical elements of the soil.

Element	Limit of Detection (%)	Concentration (%)	
		Natural Soil	Contaminated Soil
Si	0.033	50.94 ± 3.10	54.01 ± 1.97
Fe	0.001	15.97 ± 1.15	14.28 ± 2.20
Al	0.097	14.80 ± 0.77	17.06 ± 1.61
Ca	0.001	7.42 ± 0.16	5.40 ± 0.47
Na	0.71	5.04 ± 3.61	3.79 ± 0.88
K	0.002	2.17 ± 0.13	2.43 ± 0.43
Ti	0.001	2.13 ± 0.28	1.97 ± 0.23
Mg	0.165	0.96 ± 0.86	0.59 ± 0.14
Mn	0.001	0.29 ± 0.06	0.25 ± 0.07
Zn	0.001	0.28 ± 0.09	0.22 ± 0.04
	Ratios		
Ca/Si		0.15 ± 0.01	0.10 ± 0.01
Si/Al		3.44 ± 0.04	3.18 ± 0.18
Mg/Al		0.06 ± 0.05	0.03 ± 0.01

Values in the table: mean value ± standard deviation (n = 3).

3.8. Consequence of Diesel Contamination on the Shear Strength of the Soil

Figure 3 shows the changes in shear stress resistance of both natural and contaminated soils. Cohesion and internal friction angle were obtained from the failure envelop plotted for each soil condition. The cohesion of the contaminated soil decreased by 20% (from 36.7 ± 0.2 kPa to 29.2 ± 0.1 kPa), and its internal friction angle increased by 30% (from 26.9° ± 0.2° to 34.8° ± 0.1°) after soil contamination.

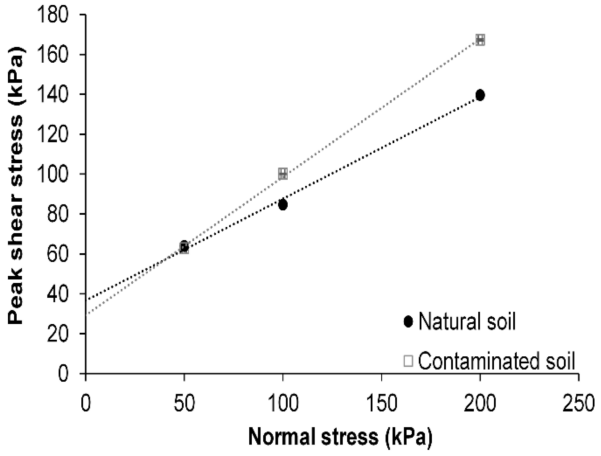

Figure 3. Effect of diesel contamination on the direct shear behavior of soil.

The cohesion of soil depends on the material type as well as the intermolecular bonds between clay particles and the absorbed water. As the natural soil particles got coated by diesel, clay particles agglomerated, formed silt-like size grains, and reduced the clay-like size grains content in the contaminated soil. Although both soils had nearly the same equivalent water content ($E_{wc-natural} = 36.94\% \pm 0.19\%$ vs. $E_{wc-contaminated} = 35.13\% \pm 0.22\%$) and saturation degree ($s_{r-natural} = 70.82 \pm 0.18$ vs. $s_{r-contaminated} = 71.28\% \pm 0.21\%$), the chemical characteristics of the diesel and soil water content reduction contributed to the decrease in the contaminated soil's cohesion.

The reduction of the soil's cohesion has been reported by other authors [5,12,13]. They attributed this decrease to reducing the specific surface area (SSA) of soil particles due to hydrocarbon deposition over the soil grains. The reduction of the SSA decreased the CEC of the soil and reduced the contact between the soil particles and water molecules [5,12,13]. Therefore, the cohesion of the soils was reduced since soil particles absorbed a lower quantity of water.

The agglomeration effect of diesel over the soil particles increased the friction angle of the contaminated soil. Thus, it can be inferred that under normal stresses between 100 and 200 kPa, contaminated soil will exhibit a higher shear resistance than natural soil. The quality of the soil is not only defined by its shear strength but also by its consolidation behavior.

So, before considering that the contaminated soil quality was enhanced due to its higher shear strength, it is necessary to consider its permeability and compressibility changes. As has already been reported, diesel deposition over soil particles reduced the soil's hydraulic conductivity [9] and SSA [12,13]. Hence, higher settlements may be observed compared to the ones obtained for the natural soil [7,12]. Furthermore, the slope stability of the trenches located over contaminated soils must be verified because of the decrease in its cohesion.

Peak shear stresses were plotted for each soil condition (Figure 3). For a normal stress of 50 kPa, natural and contaminated soils showed almost the same shear strength. However, for the 100 and 200 kPa normal stresses, the shear strength of contaminated soil was increased by 18% and 20%, respectively. According to Fredlund et al. [40], the shear strength of unsaturated soils (τ_f) can be evaluated in terms of two stress state variables, as shown in Equation (9):

$$\tau_f = c' + (\sigma_n - u_a)\, tan\phi^a + (u_a - u_w)\, tan\phi^b. \quad (9)$$

The first two terms of Equation (9) correspond to the Mohr–Coulomb criterion, c' is the effective cohesion, $(\sigma_n - u_a)$ denotes the net normal stress, u_a is the pore air pressure, and ϕ^a is the angle of frictional resistance related with normal stress. The third term of Equation (9) introduces an additional friction angle (ϕ^b) relative to matric suction ($\psi_m = u_a - u_w$) contribution to shear strength resistance, where u_w corresponds to the pore water pressure.

Total soil suction (ψ_t) considers the effect of the matric suction (ψ_m) and osmotic or solute suction (ψ_o), as expressed in Equation (10). Matric suction was defined as the difference between u_a and u_w, and is related to capillary effects. Osmotic suction arises from the presence of dissolved salts or solutes in the soil pore fluid.

$$\psi_t = \psi_m + \psi_o \quad (10)$$

The natural soil had a ψ_m of 4709 ± 1 kPa, while the contaminated soil had a ψ_m of 2077 ± 12 kPa. As the contaminated soil had a considerably lower matric suction than the natural soil, a decrease in its shear strength could be expected. This is because the tension force developed by the air–water interface or contractile skin on soil particles decreases as the matric suction decreases [41]. In contrast, an increase in shear strength of soil was observed after its contamination.

The ψ_t of natural and contaminated soils were 7521 ± 1 kPa and 18,484 ± 13 kPa, respectively. From Equation (5), the ψ_o can be obtained as the difference between ψ_t and ψ_m. As shown in Figure 4a, the ψ_m had a higher effect on the shear strength of natural soil, while the ψ_o had a major role in the shear strength of the contaminated soil (Figure 4b).

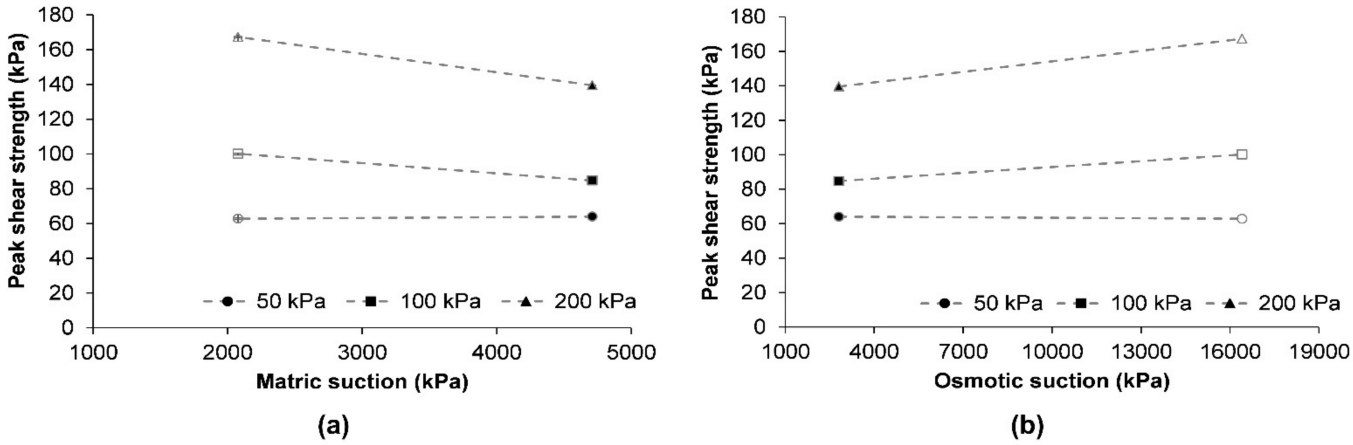

Figure 4. Influence of diesel contamination: (**a**) matric suction and (**b**) osmotic suction in the shear strength of soil. The symbols filled in black color correspond to natural soil while the symbols in grey color correspond to contaminated soil.

It is known that ψ_t influences the shear stress behavior of the unsaturated soils. However, in geotechnical engineering applications, the ψ_m component is more frequently considered than the contribution of ψ_o [41]. Nevertheless, in the case of contaminated soils, the impact of ψ_o on the shear strength of soil must be considered [42].

Therefore, as proposed by [42], and considering ψ_o as an independent stress-state variable, Equation (11) could be modified as:

$$\tau_f = c' + (\sigma_n - u_a)\, tan\phi^a + \psi_o\, tan\phi^c \quad (11)$$

where ϕ^c corresponds to the fiction angle relative to osmotic suction contribution to shear strength resistance.

Figure 5 shows the strength envelop, considering ψ_o as an independent stress-state variable, as well as the equation for shear strength behavior of the contaminated soil, according to the results obtained in this research, as a function of both normal stress and osmotic suction.

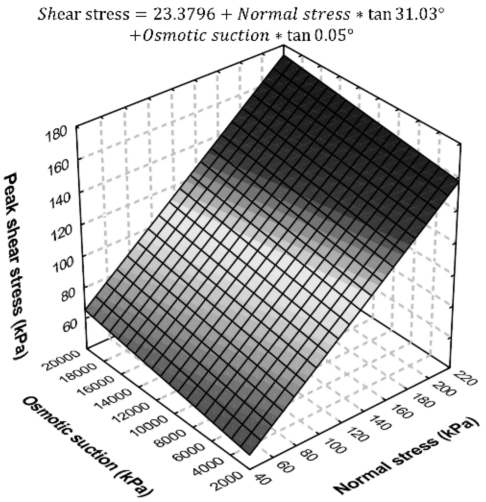

Figure 5. Contaminated soil shear strength model based on osmotic suction and normal stress.

3.9. Effect of Diesel Contamination on the Soil's Mineralogy

Figure 6 shows the X-ray diffractograms of both the natural and the contaminated soil. Both soil samples showed the presence of montmorillonite clay mineral [PDF 00-013-0135: montmorillonite-15A: $Ca_{0.2}(Al,Mg)_2Si_4O_{10}(OH)_2 \cdot 4H_2O$] and anorthite [PDF 00-018-1202: anorthite, sodian, intermediate: $(Ca,Na)(Si,Al)_4O_8$]. Montmorillonite belongs to the smectite group and is formed by two Si-based tetrahedral sheets. Anorthite is a plagioclase feldspar mineral that occurs in some igneous and metamorphic rocks.

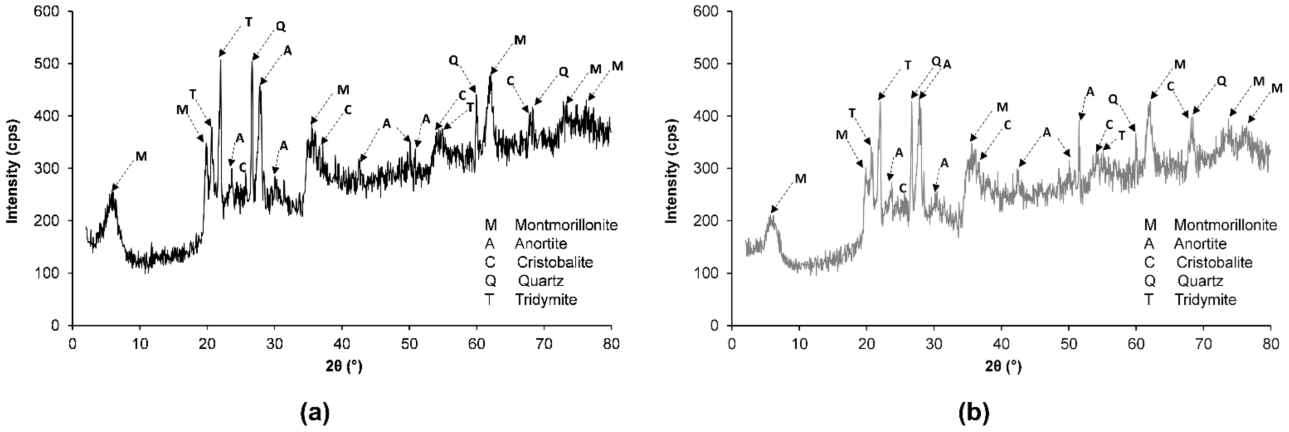

Figure 6. X-ray diffractogram of: (**a**) natural and (**b**) diesel-contaminated soils.

The presence of quartz, cristobalite, and tridymite was also observed. Silica or silicon dioxide (SiO_2) can exhibit both crystalline (quartz, tridymite, and cristobalite) and amorphous forms. Cristobalite and tridymite are silica mineral quartz polymorphs that exhibit the same chemical formula but have different crystal structures.

In most cases, cristobalite is the first crystallization product of the amorphous SiO_2 at high temperatures. In tridymite, the silica tetrahedra are packed in a two-layer structure, while in cristobalite, the silica tetrahedra are packed in a three-layer structure [43]. Cristobalite and tridymite have a more open structure than quartz, which allows the inclusion of other elements into its crystal structure [43].

A change was observed in the reflective angle of the montmorillonite in diesel-contaminated soil ($2\theta = 5.70°$) in comparison with natural soil ($2\theta = 5.88°$). This shift to the left of montmorillonite peak caused an increase in the lattice spacing of the montmorillonite mineral [44]. It implies that montmorillonite may undergo a swelling effect of the internal layer, from d_{001} = 15.018 Å (for natural soil) to d_{001} = 15.492 Å (for diesel-contaminated soil), due to its diesel contamination.

Soil contamination also decreased the peak area of the montmorillonite minerals, which was due to a reduction in the column length of the reflective minerals. This indicated a decrease in the montmorillonite minerals' concentration [44].

Although the peaks of quartz, cristobalite, and tridymite minerals did not show a shift in their reflective angle, their intensities were reduced after soil contamination. This was due to a coating effect on the mineral surface, caused by the peripheral adsorption of diesel on these minerals [44]. Such an effect resulted in an apparent decrease in the concentration of mineral crystals, since they were not able to reflect the incident X-rays as the natural soil could.

3.10. Impact of Diesel Contamination on the Chemical Elements of the Soil

The results of the analysis of the chemical elements of both natural and contaminated soils are presented in Table 6. For both soil conditions, the major elements detected were Si, Fe, Al, Ca, Na, and K, while minor elements were Mg, Mn, and Zn. In nature, inorganic exchange ions (e.g., Ca^{2+} and Na^{+}) frequently balance the clays' net negative charge [33].

Further, in clays, the hydrophilic nature of the mineral surfaces is due to the occurrence of Si–O groups and the hydration of those inorganic exchangeable ions [33].

Although the concentration of the elements detected varied from natural to contaminated condition, no significant changes were observed ($p > 0.09$), except for calcium ($p < 0.01$). The statistical analysis of this data set is presented in Appendix A. The reduction of calcium content after soil contamination was attributed to a chemical reaction with any of the diesel constituents; for example, the sulfur contained in the applied diesel. Due to the calcium concentration decrease in the contaminated soil matrix, both a pH and a cation exchange reduction can be expected [45].

3.11. Effect of Diesel Contamination on Some Properties Related with Its Possible Remediation

3.11.1. Electrical Conductivity of the Soil

The EC of soil has been used as a parameter related to the level of macronutrients and micronutrients available in the soil [46]. The EC of the natural soil decreased from 536 ± 86 µS/cm to 420 ± 38 µS/cm after its contamination. Due to this significant decrease ($p < 0.03$), it is possible that the available nutrients for both microorganisms and plants may be unbalanced, and an addition of external nutrients may be needed for soil bioremediation. The observed EC reduction has been previously reported [9], and it was attributed to the low dielectric constant of the diesel which reduced the dielectric constant of the soil's pore fluid [9].

3.11.2. Organic Matter Content in the Soil

The organic matter content of natural soil increased from 5.7% ± 0.5% to 11.6% ± 0.2% after its contamination. This increment was related to the presence of diesel in soil—no other sources of organic matter were added. Due to the organic nature of diesel, it is possible to infer that organic carbon concentration in contaminated soil also increased. Thus, the C:N:P ratio of contaminated soil has to be verified because if it is not in a suitable range, the efficiency of the available bioremediation and phytoremediation techniques may be reduced.

3.11.3. Soil's Cation Exchange Capacity

Soil's CEC is one of the factors that influence its pH buffer capacity. After soil contamination, its CEC was reduced by 50% in comparison with its CEC at its natural condition (from 75.94 to 38.41 $cmol_+/kg$). This indicates a drop in the pH buffering capacity of the contaminated soil that is reflected in its acidification because the higher the CEC capacity, the higher the pH buffering capacity [46].

Kaya and Fang [37] suggested that the decrease of the CEC was associated to the reduction of the dielectric constant of the pores' fluid, because the number of the exchangeable cations diminished when the dielectric constant of the pore fluid got reduced.

The CEC reduction indicates that contaminated soil decreased its capacity to retain and release cations, such as Ca^{2+}, Mg^{2+}, K^+, and Na^+, by electrostatic forces, in comparison with natural soil. So, a reduction in soil fertility can be expected since Ca^{2+}, Mg^{2+}, K^+, Mn^{2+}, and Fe^{2+} are considered as bioavailable metal cation species essential for green plant nutrition and soil microorganisms [47].

It is known that organic matter has a high CEC. Thus, an increase in the CEC of contaminated soil, due to the increment of its organic matter content, can be expected. However, a decreased CEC in contaminated soil was observed. When diesel was added to the natural soil, cation exchange between diesel and calcium cations (Ca^{2+}), contained in both clay minerals and organic matter, was promoted.

This process released Ca^{2+} in the soil's pores' solution that were used by clay particles to flocculate and, at the same time, to counteract the acidification effect caused by the added H^+. Thus, although the organic matter content increased in contaminated soil, it could not increase its CEC.

4. Conclusions

The geotechnical properties of unsaturated diesel-contaminated soil were evaluated and compared with the ones obtained for the soil under natural condition. Diesel concentration in the soil was gradually increased from 0% to 14%; however, the soil could only retain 12.62% ± 0.27% of the added diesel, which corresponded to a saturation rate of 79.46% ± 1.03%. This result indicated that the soil only retained the necessary diesel to fulfil its hydration demands.

Diesel contamination of soil reduced its calcium content and caused a decrease in the pH of the soil. Diesel promoted the agglomeration of fine-grain-sized particles of the soil and changed the particle size distribution of the contaminated soil.

The cohesion of contaminated soil decreased by 20%, while its internal friction angle increased by 30%. Although the matric suction of contaminated soil was considerably lower than the one obtained for natural soil; its osmotic suction was considerably higher. This contributed to an increase in the shear strength of the contaminated soil as compared to the natural soil. However, before considering that the contaminated soil quality improved due to its higher shear strength, the consolidation behavior of the contaminated soil should be assessed.

Author Contributions: Conceptualization, C.E.H.-M.; experiment set up, C.E.H.-M.; investigation, P.G.R. and C.E.H.-M.; data visualization, P.G.R. and C.E.H.-M.; writing–original draft, C.E.H.-M.; writing–review & editing, P.G.R., O.C.A. and C.E.H.-M.; project administration, C.E.H.-M.; funding acquisition, C.E.H.-M. and O.C.A. All authors have read and agreed to the published version of the manuscript.

Funding: This research was funded by the Consejo Nacional de Ciencia y Tecnología (CONACYT), grant number 270161, and by the Universidad Autónoma de Querétaro, grant number FIN-2020-03 (FONDEC-UAQ-2019).

Institutional Review Board Statement: Not applicable.

Informed Consent Statement: Not applicable.

Data Availability Statement: Data presented is contained within the article.

Conflicts of Interest: The authors declare no conflict of interest. The funders had no role in the design of the study; in the collection, analyses, or interpretation of data; in the writing of the manuscript, or in the decision to publish the results.

Appendix A

Statistical analysis of the concentration of the chemical elements of the soil reported on Table 4. The analysis was executed in Excel for Microsoft 365 with the "Data analysis" tool.

Table A1. Sodium.

Summary						
Groups	*Account*	*Sum*	*Average*	*Variance*		
Na—Natural soil	3	15.13	5.043333333	13.0270333		
Na—Contaminated soil	3	11.37	3.79	0.7761		
ANALYSIS OF VARIANCE						
Origin of variances	*Sum of squares*	*Degrees of freedom*	*Mean of squares*	*F*	*Probability*	*Critical value for F*
Between groups	2.356266667	1	2.356266667	0.3414104	0.590383	7.708647422
Within groups	27.60626667	4	6.901566667			
Total	29.96253333	5				

Table A2. Magnesium.

Summary						
Groups	*Account*	*Sum*	*Average*	*Variance*		
Mg—Natural soil	3	2.887	0.962333333	0.74157633		
Mg—Contaminated soil	3	1.768	0.589333333	0.01989033		
ANALYSIS OF VARIANCE						
Origin of variances	*Sum of squares*	*Degrees of freedom*	*Mean of squares*	*F*	*Probability*	*Critical value for F*
Between groups	0.2086935	1	0.2086935	0.54813562	0.500182374	7.708647422
Within groups	1.522933333	4	0.380733333			
Total	1.731626833	5				

Table A3. Aluminum.

Summary						
Groups	*Account*	*Sum*	*Average*	*Variance*		
Al—Natural soil	3	44.386	14.79533333	0.59737233		
Al—Contaminated soil	3	51.185	17.06166667	2.60753433		
ANALYSIS OF VARIANCE						
Origin of variances	*Sum of squares*	*Degrees of freedom*	*Mean of squares*	*F*	*Probability*	*Critical value for F*
Between groups	7.704400167	1	7.704400167	4.80787802	0.093411475	7.708647422
Within groups	6.409813333	4	1.602453333			
Total	14.1142135	5				

Table A4. Silica.

Summary						
Groups	*Account*	*Sum*	*Average*	*Variance*		
Si—Natural soil	3	152.826	50.942	9.635884		
Si—Contaminated soil	3	162.029	54.00966667	3.88626633		
ANALYSIS OF VARIANCE						
Origin of variances	*Sum of squares*	*Degrees of freedom*	*Mean of squares*	*F*	*Probability*	*Critical value for F*
Between groups	14.11586817	1	14.11586817	2.08781412	0.221990319	7.708647422
Within groups	27.04430067	4	6.761075167			
Total	41.16016883	5				

Table A5. Potassium.

Summary						
Groups	*Account*	*Sum*	*Average*	*Variance*		
K—Natural soil	3	6.521	2.173666667	0.01738433		
K—Contaminated soil	3	7.283	2.427666667	0.18305233		
ANALYSIS OF VARIANCE						
Origin of variances	*Sum of squares*	*Degrees of freedom*	*Mean of squares*	*F*	*Probability*	*Critical value for F*
Between groups	0.096774	1	0.096774	0.9656317	0.381407702	7.708647422
Within groups	0.400873333	4	0.100218333			
Total	0.497647333	5				

Table A6. Calcium.

Summary						
Groups	*Account*	*Sum*	*Average*	*Variance*		
Ca—Natural soil	3	22.247	7.415666667	0.02434433		
Ca—Contaminated soil	3	16.195	5.398333333	0.21904633		
ANALYSIS OF VARIANCE						
Origin of variances	*Sum of squares*	*Degrees of freedom*	*Mean of squares*	*F*	*Probability*	*Critical value for F*
Between groups	6.104450667	1	6.104450667	50.1617482	0.002097894	7.708647422
Within groups	0.486781333	4	0.121695333			
Total	6.591232	5				

Table A7. Titanium.

Summary						
Groups	*Account*	*Sum*	*Average*	*Variance*		
Ti—Natural soil	3	6.393	2.131	0.081003		
Ti—Contaminated soil	3	5.924	1.974666667	0.05164433		
ANALYSIS OF VARIANCE						
Origin of variances	*Sum of squares*	*Degrees of freedom*	*Mean of squares*	*F*	*Probability*	*Critical value for F*
Between groups	0.036660167	1	0.036660167	0.55274638	0.498494008	7.708647422
Within groups	0.265294667	4	0.066323667			
Total	0.301954833	5				

Table A8. Manganese.

Summary						
Groups	*Account*	*Sum*	*Average*	*Variance*		
Mn—Natural soil	3	0.878	0.292666667	0.00410233		
Mn—Contaminated soil	3	0.751	0.250333333	0.00423233		
ANALYSIS OF VARIANCE						
Origin of variances	*Sum of squares*	*Degrees of freedom*	*Mean of squares*	*F*	*Probability*	*Critical value for F*
Between groups	0.002688167	1	0.002688167	0.64505679	0.466896995	7.708647422
Within groups	0.016669333	4	0.004167333			
Total	0.0193575	5				

Table A9. Iron.

Summary						
Groups	*Account*	*Sum*	*Average*	*Variance*		
Fe—Natural soil	3	47.916	15.972	1.315753		
Fe—Contaminated soil	3	42.831	14.277	4.838479		
ANALYSIS OF VARIANCE						
Origin of variances	*Sum of squares*	*Degrees of freedom*	*Mean of squares*	*F*	*Probability*	*Critical value for F*
Between groups	4.3095375	1	4.3095375	1.40051188	0.302164965	7.708647422
Within groups	12.308464	4	3.077116			
Total	16.6180015	5				

Table A10. Zinc.

Summary						
Groups	*Account*	*Sum*	*Average*	*Variance*		
Zn—Natural soil	3	0.825	0.275	0.008757		
Zn—Contaminated soil	3	0.664	0.221333333	0.00189233		
ANALYSIS OF VARIANCE						
Origin of variances	*Sum of squares*	*Degrees of freedom*	*Mean of squares*	*F*	*Probability*	*Critical value for F*
Between groups	0.004320167	1	0.004320167	0.81134969	0.418651132	7.708647422
Within groups	0.021298667	4	0.005324667			
Total	0.025618833	5				

References

1. Johnson, S.T.; Jardine, F.M. A framework for assessing risk in contaminated land engineering. In *Contaminated Soil '95. Soil & Environment*; van den Brink, J.W., Bosman, R., Arendt, F., Eds.; Springer: Dordrecht, The Netherlands, 1995; Volume 5, pp. 1475–1486. [CrossRef]
2. Meegoda, N.J.; Ratnaweera, P. Compressibility of contaminated fine-grained soils. *Geotech. Test. J.* **1994**, *17*, 101–112. [CrossRef]
3. Rahman, Z.; Hamzah, U.; Taha, M.; Ithnain, N.S.; Ahmad, N. Influence of oil contamination on geotechnical properties of basaltic residual soil Zulfahmi. *Am. J. Appl. Sci.* **2010**, *7*, 954–961. [CrossRef]
4. Ijimdiya, T.S. The effect of oil contamination on the consolidation properties of lateritic soil. *Develop. Appl. Ocean. Eng.* **2013**, *2*, 53–59.
5. Safehian, H.; Rajabib, A.M.; Ghasemzadeh, H. Effect of diesel-contamination on geotechnical properties of illite soil. *Eng. Geol.* **2018**, *241*, 55–63. [CrossRef]
6. Heris, M.N.; Aghajani, S.; Hajialilue-Bonab, M.; Molamahmood, H.V. Effects of lead and gasoline contamination on geotechnical properties of clayey soils. *Soil Sediment. Contam.* **2020**, *29*, 340–354. [CrossRef]
7. Yazdi, A.; Teshnizi, E.S. Effects of contamination with gasoline on engineering properties of fine-grained silty soils with an emphasis on the duration of exposure. *SN Appl. Sci.* **2021**, *3*, 704. [CrossRef]
8. Correia, N.D.; Portelinha, F.H.M.; Mendes, I.S.; da Silva, J.W.B. Lime treatment of a diesel-contaminated coarse-grained soil for reuse in geotechnical applications. *Int. J. Geo-Eng.* **2020**, *11*, 8. [CrossRef]
9. Taheri, S.; Ebadi, T.; Maknoon, R.; Amiri, M. Predicting variations in the permeability and strength parameters of a sand-bentonite mixture (SBM) contaminated simultaneously with lead (II) and diesel. *Appl. Clay Sci.* **2018**, *157*, 102–110. [CrossRef]
10. Izdebska-Mucha, D.; Trzcinski, J. Effects of petroleum pollution on clay soil microstructure. *Geologija* **2008**, *50*, 69–75.
11. Son, Y.; Oh, M.; Lee, S. Influence of diesel fuel contamination on the electrical properties of unsaturated soil at a low frequency range of 100 Hz–10 MHz. *Environ. Geol.* **2009**, *58*, 1341–1348. [CrossRef]
12. Salimnezhad, A.; Soltani-Jigheh, H.; Soorki, A.A. Effects of oil contamination and bioremediation on geotechnical properties of highly plastic clayey soil. *J. Rock Mech. Geotech. Eng.* **2021**, *13*, 653–670. [CrossRef]
13. Kermani, M.; Ebadi, T. The effect of oil contamination on the geotechnical properties of fine-grained soils. *Soil Sediment. Contam.* **2012**, *21*, 655–671. [CrossRef]
14. DieselNet. Mexico: Diesel Fuel. *Fuel Regulations.* Available online: https://dieselnet.com/standards/mx/fuel.php#y2016 (accessed on 5 October 2020).
15. Villalobos, M.; Avila-Forcada, A.P.; Gutierrez-Ruiz, M.E. An Improved Gravimetric Method to Determine Total Petroleum Hydrocarbons in Contaminated Soils. *Water Air Soil Pollut.* **2008**, *194*, 151–161. [CrossRef]
16. Meegoda, N.J.; Rajapakse, R.A. Short-Term and Long-Term Permeabilities of Contaminated Clays. *J. Environ. Eng.* **1993**, *119*, 725–743. [CrossRef]
17. Meegoda, J.N.; Chen, B.; Gunasekera, S.D.; Pederson, P. Compaction Characteristics of Contaminated Soils-Reuse as a Road Base Material. Recycled Materials in Geotechnical Applications. In Proceedings of the American Society of Civil Engineers Annual Convention, Boston, MA, USA, 18–21 October 1998; Vipulanandan, C., Elton, D.J., Eds.; Geotechnical Special Publication 79. ASCE: New York, NY, USA, 1998; pp. 195–209.
18. ASTM D2216. *Test Methods for Laboratory Determination of Water (Moisture) Content of Soil and Rock by Mass*; ASTM International: West Conshohocken, PA, USA, 2019. [CrossRef]
19. ASTM D7263. *Standard Test Methods for Laboratory Determination of Density (Unit Weight) of Soil Specimens*; ASTM International: West Conshohocken, PA, USA, 2018. [CrossRef]
20. ASTM D854. *Standard Test Methods for Specific Gravity of Soil Solids by Water Pycnometer*; ASTM International: West Conshohocken, PA, USA, 2014. [CrossRef]

21. NOM-021-RECNAT-2000. Mexican Official Norm NOM-021-RECNAT-2000 That States the Specifications of Fertility, Salinity, and Classification of Soil. *Studies, Sampling, and Analysis.* Available online: http://www.ordenjuridico.gob.mx/Documentos/Federal/wo69255.pdf (accessed on 1 September 2019).
22. ASTM D6913. *Standard Test Methods for Particle-Size Distribution (Gradation) of Soils Using Sieve Analysis*; ASTM International: West Conshohocken, PA, USA, 2017. [CrossRef]
23. ASTM D1140. *Standard Test Methods for Determining the Amount of Material Finer than 75-μm (No. 200) Sieve in Soils by Washing*; ASTM International: West Conshohocken, PA, USA, 2017. [CrossRef]
24. BS EN ISO 17892-12. *Geotechnical Investigation and Testing. Laboratory testing of soil. Determination of Liquid and Plastic Limits*; British Standards Institution/International Organization for Standardization: London, UK, 2018.
25. ASTM D2487. *Standard Practice for Classification of Soils for Engineering Purposes (Unified Soil Classification System)*; ASTM International: West Conshohocken, PA, USA, 2017. [CrossRef]
26. Sridharan, A.; Rao, S.M.; Murthy, N.S. Free swell index of soils: A need for redefinition. *Indian Geotech. J.* **1985**, *15*, 94–99.
27. ASTM D3080. *Standard Test Method for Direct Shear Test of Soils Under Consolidated Drained Conditions*; ASTM International: West Conshohocken, PA, USA, 2011. [CrossRef]
28. ASTM D5298. *Standard Test Method for Measurement of Soil Potential (Suction) Using Filter Paper*; ASTM International: West Conshohocken, PA, USA, 2016. [CrossRef]
29. AASHTO T 267. *Standard Method of Test for Determination of Organic Content in Soils by Loss on Ignition*; American Association of State Highway and Transportation Officials: Washington DC, USA, 2018.
30. Yong, R.N.; Rao, S.M. Mechanistic evaluation of mitigation of petroleum hydrocarbon contamination by soil medium. *Can. Geotech. J.* **1991**, *28*, 84–91. [CrossRef]
31. Annandarajah, A.; Chen, J. Van der Waals attractive forces between clay particles in water and contaminants. *Soils Foundations.* **1997**, *37*, 27–37. [CrossRef]
32. Chiou, C.T.; Shoup, T.D. Soil sorption of organic vapors and effects of humidity on sorptive mechanism and capacity. *Environ. Sci. Technol.* **1985**, *19*, 1196–1200. [CrossRef]
33. Lee, J.-F.; Mortland, M.M.; Chiou, C.T.; Kile, D.E.; Boyd, S.A. Adsorption of benzene, toluene, and xylene by two tetramethylammonium-smectites having different charge densities. *Clays Clay Minerals.* **1990**, *38*, 113–120. [CrossRef]
34. Alexander, M.A. *Biodegradation and Bioremediation*, 2nd ed.; Academic Press: New York, NY, USA, 1999.
35. Moeni, M.; Bayat, M.; Ajalloeian, R. Laboratory investigation on the effects of pH induced changes on geotechnical characteristics of clay soil. *Geomech. Geoeng.* **2020**. [CrossRef]
36. Mitchell, J.K.; Soga, K. *Fundamentals of Soil Behavior*, 3rd ed.; John Wiley & Sons: New York, NY, USA, 2005.
37. Kaya, A.; Fang, H.-Y. The effects of organic fluids on physicochemical parameters of fine-grained soils. *Can. Geotech. J.* **2000**, *37*, 943–950. [CrossRef]
38. Lambe, T.W.; Whitman, R.V. *Soil Mechanics*; John Wiley & Sons: New York, NY, USA, 1969.
39. Wang, Q.; Tang, A.M.; Cui, Y.-J.; Delage, P.; Gatmiri, B. Experimental study on the swelling behaviour of bentonite/claystone mixture. *Eng. Geol.* **2012**, *124*, 59–66. [CrossRef]
40. Fredlund, D.G.; Morgenstern, N.R.; Widger, R.A. The shear strength of unsaturated soils. *Can. Geotech. J.* **1978**, *15*, 313–321. [CrossRef]
41. Fredlund, D.G.; Rahardjo, H.; Fredlund, M.D. *Unsaturated Soil Mechanics in Engineering Practice*; John Wiley & Sons: New York, NY, USA, 2012.
42. Zhang, Z.; Chen, Y.; Fang, J.; Guo, F. Study on shear behavior of kaolinite contaminated by heavy metal Cu (II). *Environ. Sci. Pollut. Res.* **2019**, *26*, 13906–13913. [CrossRef]
43. Gutiérrez-Castorena, M.C. Pedogenic siliceous features. In *Interpretation of Micromorphological Features of Soils and Regoliths*, 2nd ed.; Stoops, G., Marcelino, V., Mees, F., Eds.; Elsevier: Amsterdam, The Netherlands, 2018; pp. 127–155. [CrossRef]
44. Alazigha, D.P.; Indraratna, B.; Vinod, J.S.; Heitor, A. Mechanisms of stabilization of expansive soil with lignosulfonate admixture. *Transport. Geotech.* **2018**, *14*, 81–92. [CrossRef]
45. Frenkel, H.; Suarez, D.L. Hydrolysis and decomposition of calcium montmorillonite. *Soil Sci. Soc. Am. J.* **1997**, *41*, 887–891. [CrossRef]
46. Ujowundu, C.O.; Kalu, F.N.; Nwaoguikpe, R.N.; Kalu, O.I.; Ihejirika, C.E.; Nwosunjoku, E.C.; Okechukwu, R.I. Biochemical and physical characterization of diesel petroleum contaminated soil in southeastern Nigeria. *Res. J. Chem. Sci.* **2011**, *1*, 57–62.
47. Sposito, G. *The Chemistry of Soils*, 3rd ed.; Oxford University Press: New York, NY, USA, 2016.